We are IntechOpen,
the world's leading publisher of
Open Access books
Built by scientists, for scientists

6,900
Open access books available

186,000
International authors and editors

200M
Downloads

154
Countries delivered to

Our authors are among the

TOP 1%
most cited scientists

12.2%
Contributors from top 500 universities

BOOK CITATION INDEX
CLARIVATE ANALYTICS
INDEXED

WEB OF SCIENCE™

Selection of our books indexed in the Book Citation Index
in Web of Science™ Core Collection (BKCI)

Interested in publishing with us?
Contact book.department@intechopen.com

Numbers displayed above are based on latest data collected.
For more information visit www.intechopen.com

Laser Micromachining for Gallium Nitride Based Light-Emitting Diodes

Kwun Nam Hui and Kwan San Hui

1. Introduction

Micromachining with nanosecond laser pulses is a powerful tool that is suitable for replacing or complementing traditional wafer processes, such as dicing and etching, as well as advanced process developments, such as laser lift-off [1], laser-assisted machining [2] and medical and biotechnology research [3]. Tightly-focused nano-second laser pulses can enable micromachining with much higher precision and dimensions down to several micrometers [4]. For more advanced applications, micromachining parameters, such as laser wavelength, pulse energy, repetition rate and pulse duration, should be considered seriously. Drilling and cutting with nanosecond, or even femtosecond ultraviolet (UV) laser pulses has been reported to produce very small heat-affected zones (HAZ) [5]. Recently, laser micromachining is being adopted gradually for gallium nitride (GaN)-based light-emitting diodes (LEDs). Because epitaxial GaN layers are typically grown on sapphire, the separation of fabricated LED dies is commonly achieved by wafer sawing, which is slow and expensive. The use of high energy laser pulses increases the process efficiency and enables a high packing density of chips through the reduced dimensions of the scribe lanes.

One of the typical configurations of laser micromachining relies on the laser scanner head, which steers the beam into the incident direction. Although it is relatively fast, mechanical vibrations tend to be magnified, resulting in a loss of pattern resolution. Alternatively, the sample to be micro-machined can be mounted onto a precision motorized translation module while the optical beam remains static, which is more suitable for processing the optical microstructures. In a conventional laser micro-machining setup for wafer dicing, the focused laser beam is incident perpendicular to the sample to be processed, so that only two dimensional patterns can be generated and vertical cuts can be obtained. Projecting the beam at an oblique angle to the sample enables three-dimensional micromachining. Nevertheless, it

cannot mount the translation module at a tilted angle because it will result in severe beam distortion. In the proposed approach, a laser beam turning mirror was introduced to the optical path to achieve a continuously-tunable range of tilting angles for beam projection, while retaining the beam quality. Laser micromachining is a potential simple, inexpensive and high-throughput alternative method for creating geometrically-shaped GaN LEDs compared to other available technologies [6,7,8]. K.N. Hui et al. reported the effectiveness of laser micro-machining incorporated with GaN semiconductors to achieve high light extraction GaN LEDs [7,9] and color tunable vertically-stacked LEDs in solid-state lighting applications [7,10].

This chapter examines the experimental process of laser micromachining, and the structural and optical properties of laser micromachining LED chips with a range of geometries. The optical characterization of LED, particularly the light extraction efficiency of geometrically-shaped LEDs, is discussed because the light extraction efficiency plays an important role in achieving high luminous efficacy LEDs. Finally, several applications derived from the utilization of laser micromachining, e.g. geometrically-shaped LED, angularly uniform white LEDs, and vertically-stacked polychromatic LEDs are presented.

2. Process of laser micromachining

One attractive feature of laser processes is its ability to remove material. Termed laser ablation, material removal can be achieved by physical or chemical microscopic mechanisms. Because lasers can be focused on a small spot with high energy density, precision machining of the features on the micrometer or tens of micrometer scale is possible. For example, E. Gu et al. examined the drilling of holes and micro-trenches in a free-standing GaN substrate by pulsed UV laser ablation[4]. Another use of laser ablation in LED industries is wafer dicing. As GaN is normally grown on sapphire, and sapphire is the second hardest material in the world, a diamond blade is the only viable tool for mechanical dicing. On the other hand, a diamond blade often deviates from its intended dicing direction when the blades are thin, causing chipping or even device damage. With laser dicing, the dicing path can be controlled with high precision. In addition, the spacing between the individual LED dies can be reduced to a size comparable to the laser spot size, leading to an increase in die density.

Simple laser micromachining consists of a UV laser source, beam focusing optics and an x-y motorized translation stage, as shown in Figure 1. The laser source is a third harmonic ND:YLF diode-pumped solid state (DPSS) laser manufactured by Spectra Physics. The laser emits at 349 nm, and the pulse repetition rate ranges from single pulse to 5 kHz. At a reference diode current of 3.2 A, the pulse energy is 120 μJ at a repetition rate of 1 kHz, with a pulse width of approximately 4 nanoseconds. The TEM00 beam allows for tight focusing, offering a high spatial resolution. After beam expansion and collimation using a beam expander, the laser beam is reflected 90° using a dielectric laser line mirror and is focused onto the horizontal machining plane to a very tiny spot, several micrometers in diameter, with a focusing triplet. All optics used are made from UV-fused silica and are anti-reflection (AR) coated. The additional feature of this set-up, as illustrated in the schematic diagram of Figure 1, is the

insertion of a UV mirror at an oblique angle within the optical path between the focusing optics and machining plane, which deflects the convergent beam to strike the sample at an oblique angle to the horizontal working plane. The size of the beam at the focal point is not only limited by the capability of the UV objective lens but is also sensitive to the coaxiality of the optics. With this modified set-up, it is relatively easy to optimize and monitor the beam through the tube lens imaged with a CCD camera. Once the optical setup is optimized before inserting the tilting mirror, the mirror can be inserted without affecting the coaxiality of the laser beam, so that the dimensions of the beam spot are unaffected.
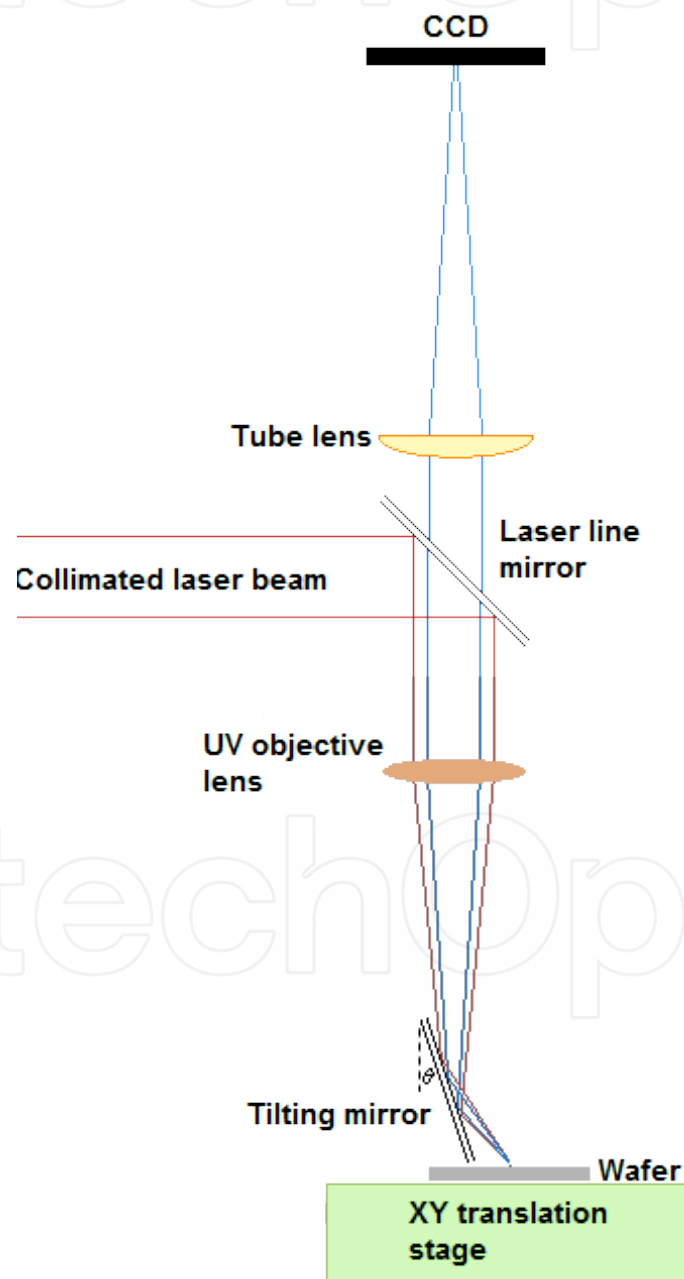

Figure 1. Experimental setup of laser micro-machining.

The angle of incidence of the deflected laser beam on the wafer is 2θ, where θ, as indicated in Figure 1, is the angle between the plane of the mirror and the normal. This angle can be precisely adjusted by mounting the mirror onto a rotation stage. Therefore, the incident angle can be varied over a wide range. In this experiment, a UV objective with a focal length of 75 mm was used based on two considerations. First, the focal length should be long enough to accommodate the mirror in the optical path. Secondly, an ideal tool for the fabrication of microstructures should have a very long penetration depth and negligible lateral dispersion. Nevertheless, an objective lens with a longer focal length also produces a larger focused beam spot. The two parameters are related by the following equation:

$$d = \frac{4\lambda M^2 f}{\pi D}$$
(1)

where M^2 quantifies the beam quality, λ is the wavelength of the laser beam, f is the focal length and D is the diameter of the incident beam.

3. Characterization of laser micromachining

3.1. Depth of micro-trenches as a function of the scan cycles

After laser micromachining, the depth of the micro-trenches pattern can be observed by scanning electron microscopy (SEM) to check the effectiveness of the approach. The quality of the cleave can be quantified by the width, depth, linearity and sidewall roughness of the trench formed by the laser beam. Because the focal length of the focusing lens (f = 75 mm) is much longer than the thickness of the GaN layer on the sapphire wafer (t = 420 μm), the depth of the trench depends mainly on the number of micromachining cycles. The number of cycles is controlled by configuring the translation stage to repeat its linear path several times. As the position reproducibility of the stage is better than 5 μm, increasing the number of cycles should not contribute significantly to the width of the feature. X.H. Wang et al. [11] reported the cross-sectional optical image of a GaN layer on a 420 μm thick sapphire wafer that had been micro-machined with an incident beam inclined at 45° with scan cycles ranging from 1 to 10. These incisions were carried out by setting the laser pulse energy to 54 μJ at a repetition rate of 2 kHz. Figure 2 shows the relationship between the inclined cutting depth and the number of passes of the beam. After the first pass of the beam, a narrow trench with a width of ~20 μm and depth of ~220 μm was formed. Successive scans of the beam along the trench resulted in further deepening and widening but the extent was increased at a decreasing rate. The depth of the trench depends on the effective penetration of the beam. From the second scan onwards, the beam needs to pass through the narrow gap before reaching the bottom of the trench for further machining. The energy available at this point was attenuated, which is partly due to lateral machining of the channel (causing undesirable widening), absorption and diffraction effects. Therefore, the depth of the trench tends to saturate after multiple scans.
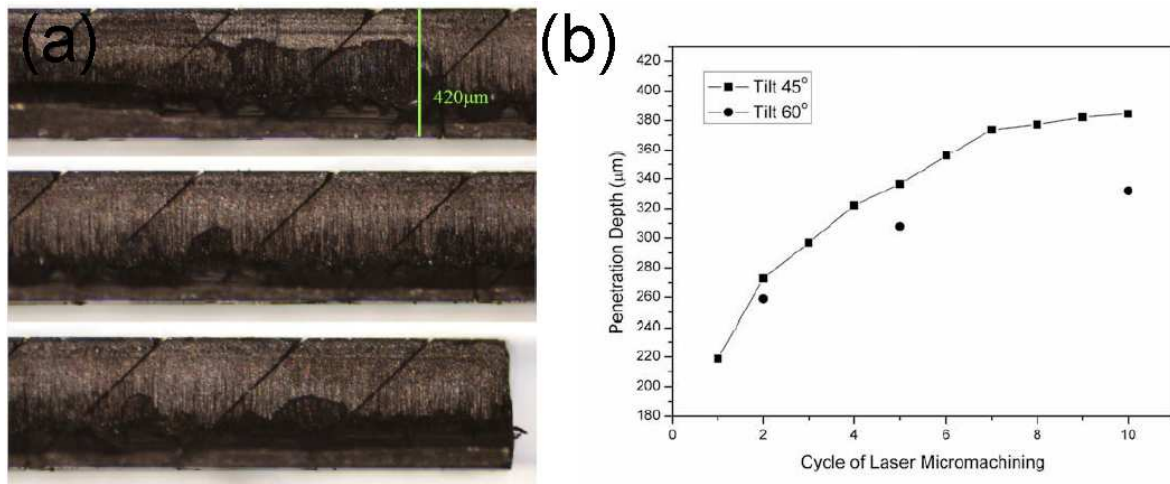
Figure 2. (a) Cross-sectional optical micrograph of laser micro-machined micro-trenches at an inclination angle of 45° at a range of scan cycles of between 1 and 10 (left to right then down), and (b) depth of tiling micro-trenches as a function of the scan cycles.

3.2. Topography of laser micromachining

In addition to the scan speed and number of scan cycles, the focus offset and pulse energy are two important parameters controlling the quality and topography of the micro-trenches of GaN structures. The focus offset level is defined as the distance shifted away from the focal plane; the downward direction is positive. Y.H. Mak et al. [12] showed that micro-trenches with different topographies can be obtained precisely by controlling the focus offset and pulse energy of the laser beam. For example, in Figure 3(a), the sample is positioned near the focal plane (300 μm from focal plane); the laser beam ablates both the GaN and sapphire layers. A V-shaped valley is formed in the sapphire layer due to the Gaussian beam shape. At the optimal focal offset plane of 450 μm, as shown in Figure 3(b), ablation terminates automatically at the GaN/sapphire interface because the laser fluence decreases below the ablation threshold value for sapphire, resulting in the exposure of a flat and smooth sapphire bottom surface. At a larger focus offset plane of 600 μm, the GaN layer is not removed completely, leaving a shallow and rugged trench on the surface (Figure 3(c)).

Figure 3(d-f) illustrates the laser micromachined micro-trenches formed at three different pulse energies (45, 23, and 7 μJ) with the other parameters constant, and the focus offset is kept at the optimal value of 450 μm. When the pulse energy is set to 45 μJ, GaN and sapphire are ablated to form a V-shaped trench (Figure 3(d)), which is similar to that with a smaller focus offset. On the other hand, a low pulse energy results in shallow micro-trenches, which is similar to the large focus offset.
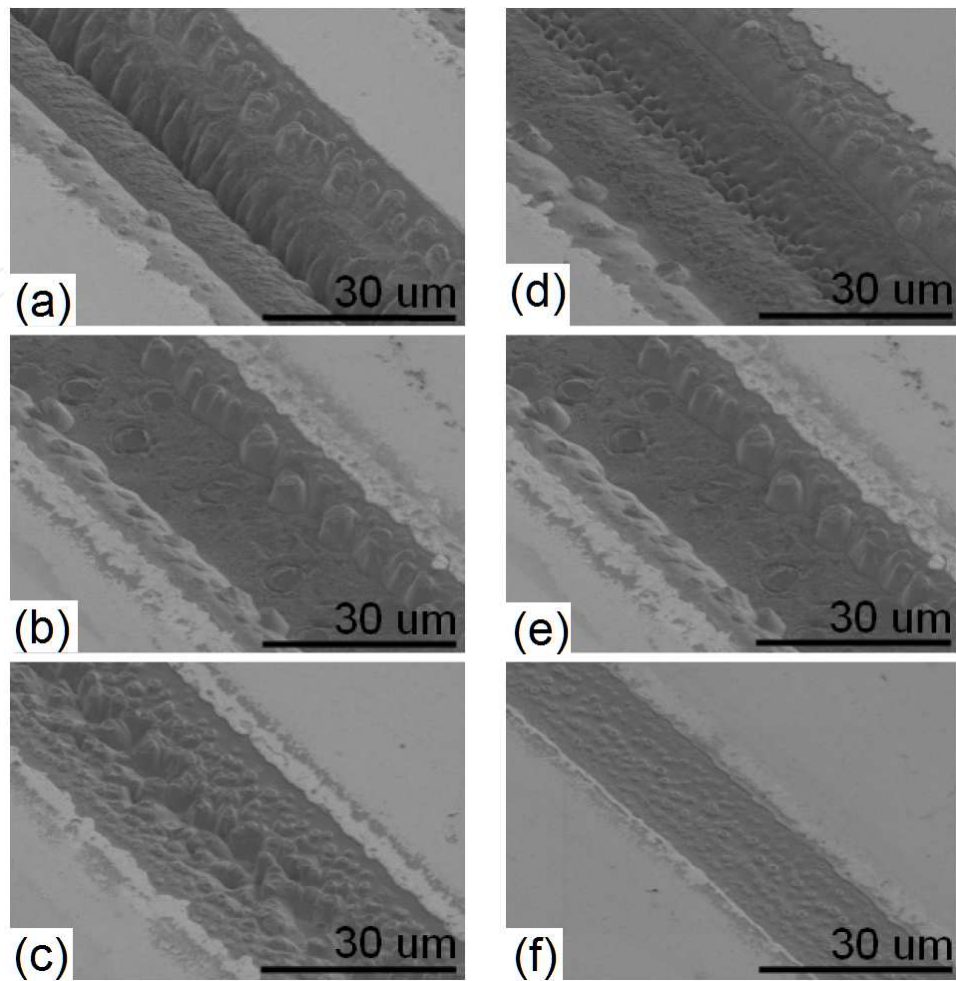
Figure 3. SEM images of micro-trenches formed by laser micromachining at different focus offset planes (with the pulse energy, pulse repetition rate and scan speed fixed at 23 µJ, 1 kHz, and 25 µm/s, respectively.): (a) small offset of 300 µm; (b) optimal offset of 450 µm; (c) large offset of 600 µm, and (d) pulse energy of 45µJ, (e) 23 µJ, and (f) 7 µJ (with the focus off-set level, pulse repetition rate, and scan speed are fixed at 450 µm, 1 kHz, and 25 µm/s, respectively.)

4. Laser micromachining applications

4.1. Geometrical shaped LED

The development of LEDs with high optical output power has been the driving force of next generation solid-state lighting [13]. On the other hand, the optical output power of the-state-of-art LEDs is still insufficient for making them practically viable. The large refractive index difference between nitride material ($\eta_{GaN} = 2.585$) and air ($\eta_{Air} = 1$), giving rise to a total internal reflection at the interfaces, is the major cause for the lower-than-expected light extraction efficiency. In addition, conventional LED chips with a cuboid geometry and a Lambertian emission pattern often have a light extraction efficiency of < 20%. Several methods have been proposed to alleviate these issues, such as flip-chip LEDs [14], photonic crystals [15] and surface texturing [16]. These proposed methods, however, are energy consuming, low

throughput, and often utilize expensive equipment, highlighting the need to search for alternative low cost methods that can be fully adopted in industrial mass production and enhance the light output intensity of LEDs significantly. Recently, the effect of geometrical chip-shaping realized with laser micromachining or other methods is being gradually recognized as a promising alternative technique for optimizing the efficiency and for modulating the emission pattern [17]. W.F. Fu et al. [8] reported that the geometrical shaping of LEDs by laser micromachining is an effective approach for enhancing the light extraction efficiency of a conventional cuboid LED (inclination angle of 90°) of 18.3% up to 33.9% in truncated pyramidal (inclination angle of 50°) LED geometry. This approach offers significant increases in light extraction efficiency of up to 85.2%, which is the highest value reported thus far.

Figure 4(a) presents the mechanism of enhanced light extraction with tiled sidewalls, showing the additional light extraction channel from the top surface as well as from the sidewalls due to reflections on the tilted sidewalls. According to the ray-tracing simulation, the light extraction efficiency depends on the inclination angle. Figure 4(b) shows the light extraction efficiency as a function of the inclination angle. Figure 4(c) shows a SEM image of an InGaN LED die with a truncated pyramidal geometry (TP-LED) fabricated by laser micromachining. Figure 5(a) and 5(b) show the operation images of a cuboid LED and a TP-LED, respectively, and Figure 5(c) presents their light output–current (*L-I*) characteristics. At lower driving currents (50 mA), the average light enhancement factor was 88.6%, which is consistent with the theoretical prediction of 85.2%. Such significant improvement in light extraction efficiency highlights the effectiveness of geometrical chip-shaping, particularly with the present approach based on laser micromachining.

4.2. Angularly uniform white LED

White LEDs are used widely in commercial applications, such as solid-state lighting, liquid crystal display (LCD) backlighting and signaling, owing to their energy efficiency and mercury-free composition. Currently, color down-conversion and color-mixing are the two mainstream methods of producing white LEDs. The use of phosphors as a conversion agent is used widely in commercial products. Nevertheless, the limited conversion efficiency from shorter wavelengths (typically blue at approximately 470 nm) to a longer wavelengths means the benefits of LEDs can never be fully achieved. Placing three LEDs (red, green and blue) into a single package (the RGB approach) resolves this deficiency but introduces severe issues with color uniformity and homogeneity. For phosphor-coated LEDs, the placement and method of the phosphor coating will also affect the color uniformity considerably, whereby emission homogeneity is an important attribute for many applications. For example, the phosphor coating process went through a reflow process to cover both the top and sidewalls, resulting in a non-uniform distribution and coating thickness, particularly at the edge of the chip. Such coating thickness non-uniformity, coupled with the unequal light emission from the top and sidewall, results in a non-uniformity of color emission from different viewing angles [18]. Therefore, tailoring the light emission pattern from the point of view of geometrically-shaped LED plays an important role in achieving high angular color uniformity. L. Zhu et al. [19] found that a truncated cone (TC) structure integrating an Al mirror reflectors on the sidewall and bottom surfaces is an effec-

tive approach for improving the angular color uniformity of white LEDs, showing 37% enhancement in color uniformity, compared to the conventional cuboid structure. Figure 6 presents three different coating profiles, phosphor-slurry coating, conformal coating and remote phosphor coating, along with the proposed white LED employing a TC structure.
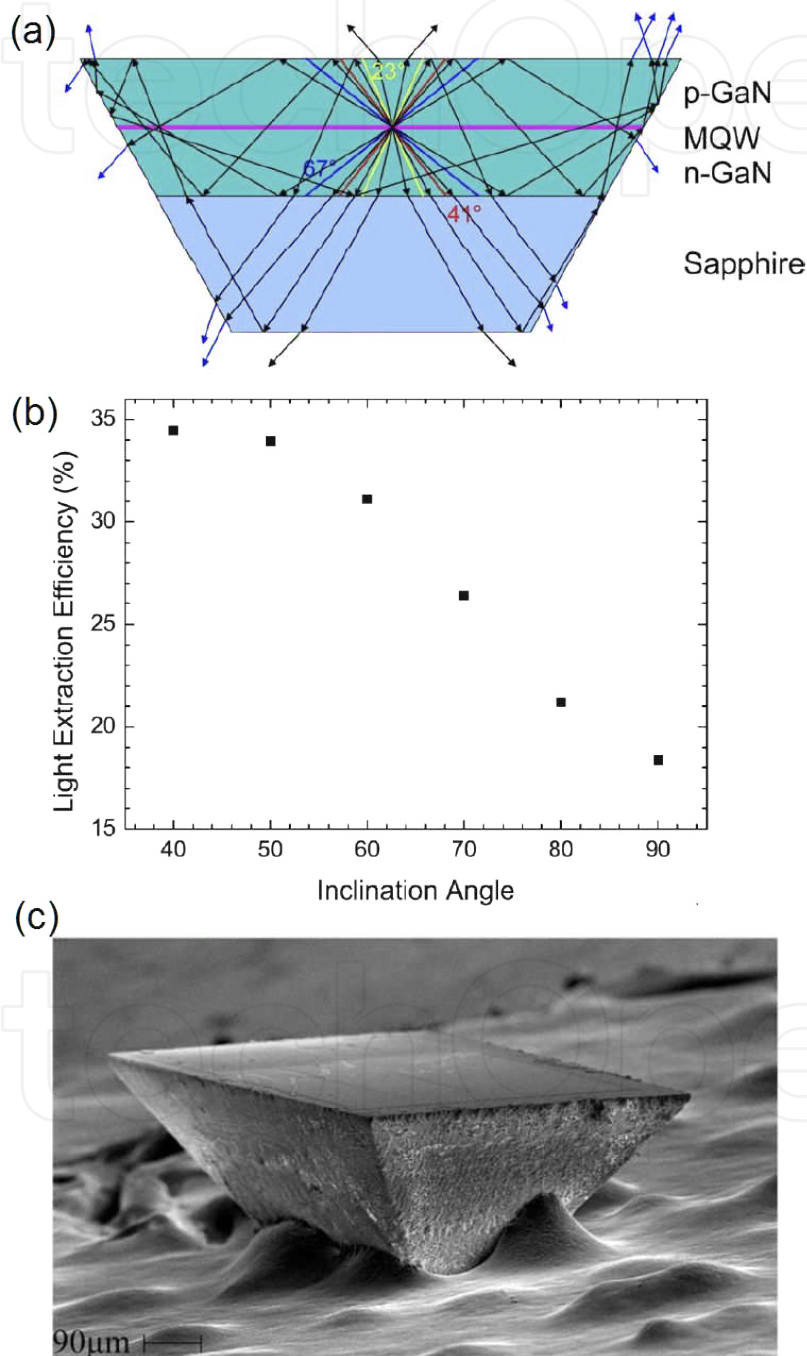

Figure 4. a) Schematic diagram showing an exemplary light ray within a TP-LED. The arrows in blue indicate the additional extracted rays due to the inclined sidewalls. (b) Light extraction efficiency of an inclined sidewall LED as a function of the inclination angle of the sidewall. (c) SEM image of an InGaN LED die with a truncated pyramidal geometry.
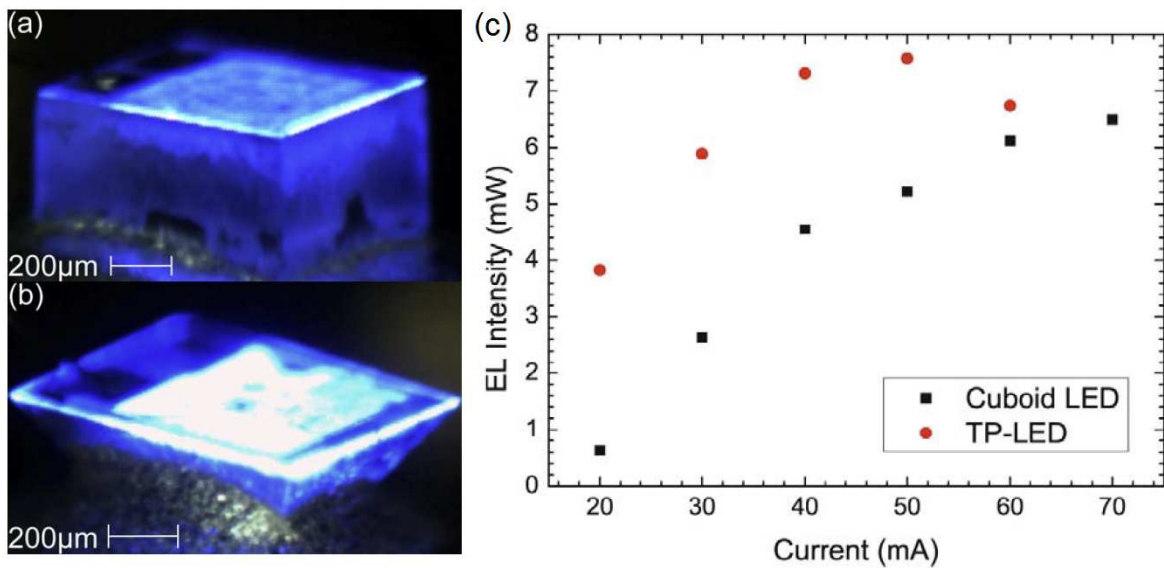
Figure 5. Optical micrographs showing cuboid LED (a) and TP-LED (b) biased at 10 mA, and (c) L-I curve comparing the performances of the TP-LED and cuboid LED.
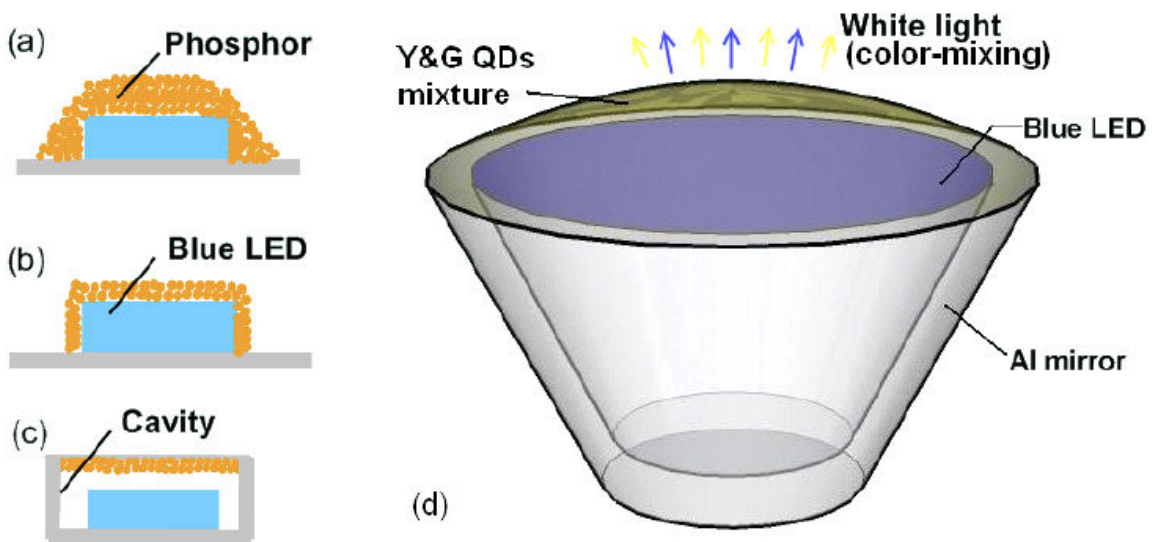

Figure 6. Schematic diagram showing the cross-sectional views of LED coating using three different methods: (a) phosphor-slurry coating; (b) conformal coating; (c) remote phosphor coating; and (d) 3D schematic diagram of a TC-LED.

Figure 7 shows operational images of a TC-LED, together with the reference LED (circular LED without TC structure). Quantum dots (QDs) consisting of green (540 nm) and yellow (560 nm) light-emitting QDs (Evident Technologies) are used as color-conversion agents, which are mixed together to a 7 : 5 volume ratio for balanced white light emission. The mixture is then blended with a transparent UV epoxy (Norland 61), following which a small volume of the slurry is dispensed onto the chips. The chips are packaged into standard TO-cans. To minimize these effects, the epoxy is spin-coated onto the chips to ensure evenness of the coating. The completed devices were tested at a bias current of

20 mA. Figure 7(c) and 7(e) shows the emission from the reference LED structure from two different angles. A ring of yellow light is clearly observed at the periphery of the circular chip, which was attributed to the relatively thicker coating on the sidewalls. This effect is suppressed with the TC-LED structure, as shown in Figure 7(d) and 7(f), where uniform white light emission can be observed from different angles.
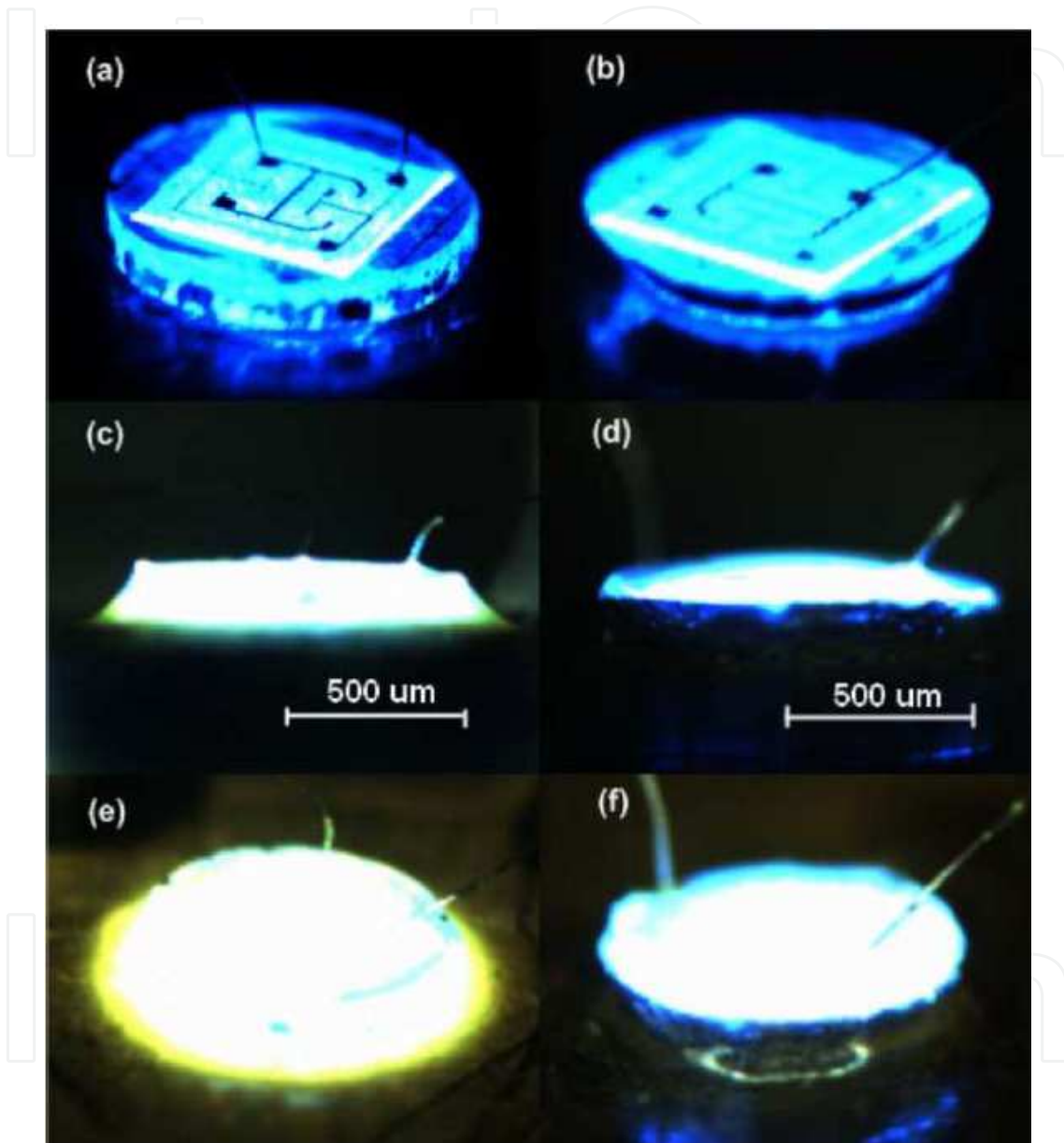

Figure 7. Operational images of the packaged devices: (a) and (b) are the circular reference LED and TC-LED; (c) and (e) show the QD-coated circular reference LED, (d) and (f) show the QD-coated TC-LED.

4.3. Vertically-stacked polychromatic LED

Recent advances in the performance of high power LEDs have led to the development of novel illumination sources with added functionality and intelligence. These advanced technologies

have attracted attention from both academia and industry due to the increasing demand for dynamic lighting not only for outdoor activities, such as accent and task lighting, stage and studio, but also in indoor activities, such as tunable interior mood lighting [20]. Numerous spectral conversion schemes have been adopted for polychromatic LEDs, such as phosphors [21], polymer dyes [22] and CdSe/CdS quantum dots [23] for color down-conversion. These schemes, however, inevitably suffer from energy loss due to Stokes shift in the conversion processes, as well as scattering losses associated with the particles. Another conversion-free approach involves the combination of three discrete LED chips of the primary colors red (R), green (G) and blue (B) arranged side-by-side on the same plane to generate a polychromatic spectrum. On the other hand, challenges exist in uniform color mixing, both spatially and angularly in such configurations [24]. K.N. Hui et al. [7,10] pioneered the stacking of TP-LED chips in that instead of placing the RGB chips onto the same plane, the individual LEDs were arranged in a vertically-stacked configuration to produce LED-stacks. The LED-stacks consisted of an InGaN/GaN blue LED (470 nm) stacked onto an InGaN/GaN green LED (520 nm), which is subsequently stacked onto an AlGaInP/GaAs red LED (650 nm). Such a stacking strategy ensures optimal color mixing and minimal absorption losses. Figure 8 provides a schematic diagram of the proposed device.
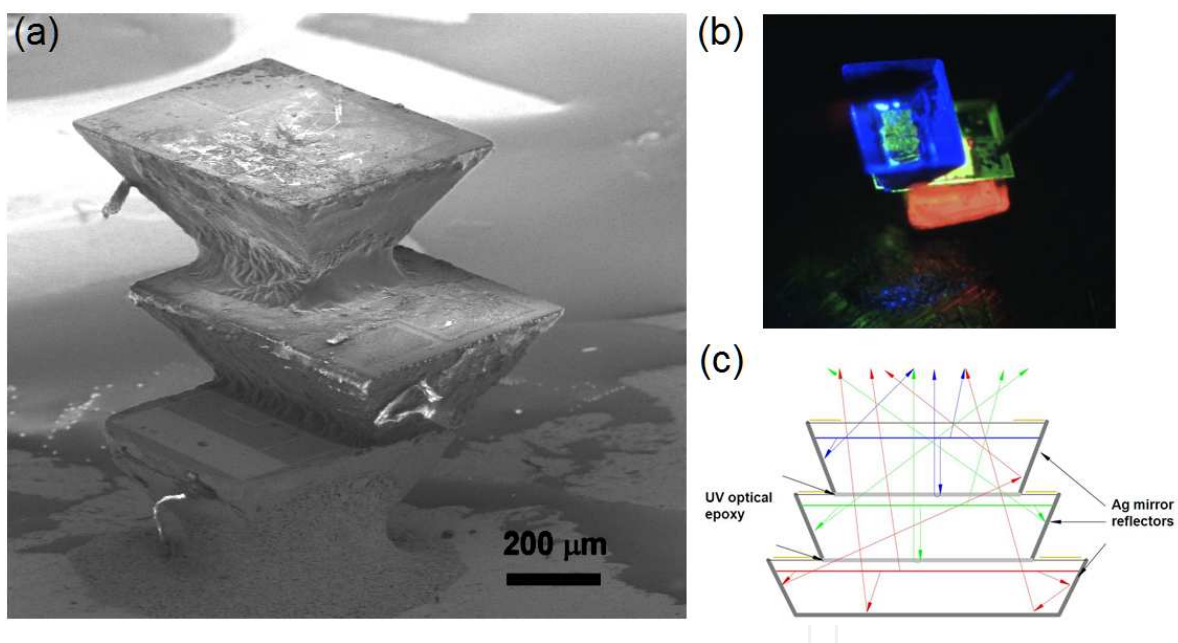

Figure 8. (a) SEM image of an LED-stack assembled from LED chips with a truncated pyramid geometry, (b) operational image of the LED-stacks, and (c) schematic diagram showing the mixing of light inside the LED-stacks.

Figure 9 shows the corresponding electroluminescence (EL) spectral data and optical emission images of the LED-stacks driven at the tested voltage combinations. A wide range of colors can be obtained from the stacked LEDs, which depend on the choice of the individual LED chip with a specific wavelength and spectral bandwidth. The proposed LED-stacks with a color tunable function have potential applications in high-resolution panel displays. Table 1 summarizes the combinations of an applied driving current for

generating a range of colors. In this study, the overall performance of the packaged stacked LEDs device was measured in a calibrated 12-inch integrating sphere. The optical signal was channeled using an optical fiber to an optical spectrometer. At a total driving current of 20 mA, the LED-stacks produced a luminous efficacy of 33 lm/W, whereas the commercial RGB LEDs produced a luminous efficacy of 30 lm/W. The corresponding CIE coordinates, CRI and CCT values of the LED-stacks were (0.32, 0.33), 69, and 6300 K, respectively, which is a promising result for a prototype device.
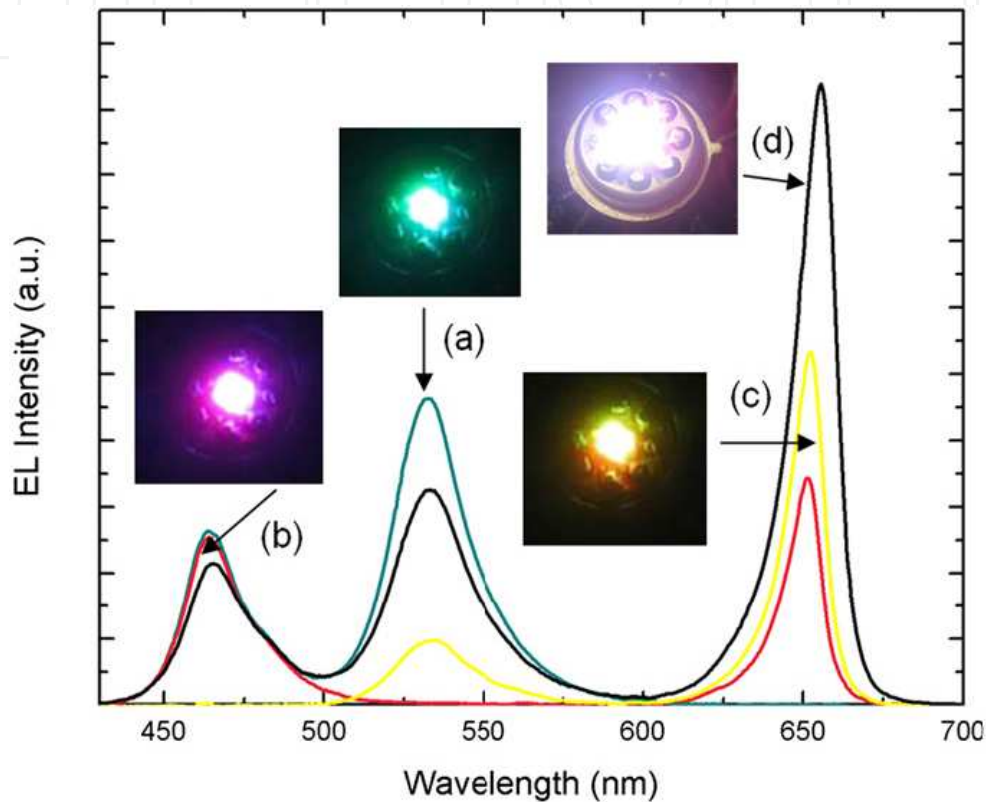

Figure 9. (a)-(d) illustrates the electroluminescence spectrum of the various colors emitted by the LED-stacks. The inserted images show the corresponding devices.

Curve	Red LED	Green LED	Blue LED	CIE (x,y)
(a)		2.57 V (2 mA)	2.70 V (10 mA)	(0.18, 0.27)
(b)	2.60 V (2 mA)		2.53 V (2 mA)	(0.31, 0.13)
(c)	2.97 V (5 mA)	2.61 V (2 mA)		(0.46, 0.53)
(d)	3.72 V (14 mA)	2.68 V (4 mA)	2.53 V (2 mA)	(0.32, 0.33)

Table 1. Biased voltage (current) of the electroluminescence spectrum for Figure 9(a) to (d).

Figure 10 shows the CIE chromaticity as a function of the viewing angle of the LED-stacks and commercial RGB LED. The CIE coordinates of light emission collected at the normal incidence (0°) from the top of the LED-stacks and the commercial RGB LEDs were

(0.32, 0.33) and (0.33, 0.33), respectively. As the angle of observation was increased from 0°
to 70 in 10° increments, shifting of the CIE coordinate from the stacked LEDs was insignif‐
icant and the device emitted mixed white light. On the other hand, under the same test,
the CIE coordinate of the commercial RGB LED shifted to a yellowish white. At an
observation angle of 70°, the farthest shift of the CIE coordinate away from the initial CIE
coordinates of the stacked LEDs was (0.29, 0.29), whereas the CIE coordinate of the
commercial RGB LED were shifted to (0.41, 0.39). These results highlight the effectiveness
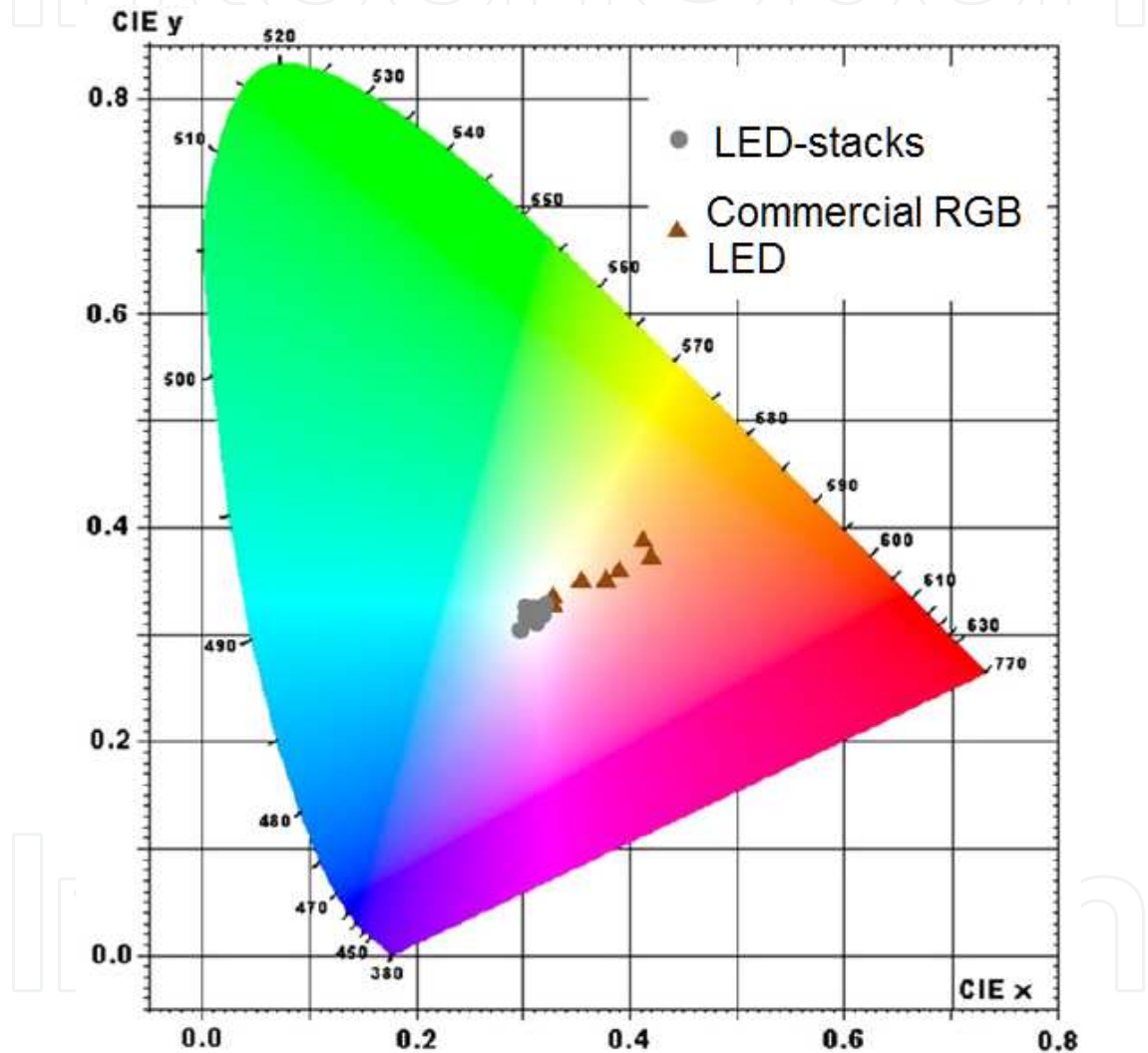of the vertical stacking of LEDs in achieving uniform color mixing.

Figure 10. Angular dependence of the CIE chromaticity on the LED-stacks and commercial RGB LED.

5. Summary

This chapter reviewed several studies of laser micromachining on GaN LEDs. Based on the
knowledge of several key parameters, such as the scan cycle, scan speed, pulse energy, and

offset focus of laser micromachining, laser micromachining is a feasible approach for obtaining high quality and performance GaN LEDs. On the other hand, a few laser micromachining applications have been addressed. Geometrically-shaped LEDs provides an effective way of enhancing the light extraction efficiency of LEDs. Angularly uniform white LEDs help improve the angular color uniformity of white LEDs. Vertically-stacked polychromatic LEDs can improve light extraction and has potential applications including high uniformity color-tunable light sources and conversion-free white LED. The mass production of high light extraction efficiency LEDs, high angular color uniformity white LEDs and high functionality GaN-based LEDs may be realized in the near future when the laser micromachining approach is adopted widely.

Acknowledgements

Author details

Kwun Nam Hui[1*] and Kwan San Hui[2,3]

*Address all correspondence to: bizhui@pusan.ac.kr; kwanshui@um.cityu.edu.hk

1 Department of Materials Science and Engineering, Pusan National University, Geumjeong-Gu, Busan, Republic of Korea

2 Department of Systems Engineering & Engineering Management, City University of Hong Kong, Kowloon Tong, Hong Kong, China

3 Department of Mechanical Engineering, Hanyang University, Seongdong-gu, Seoul, Republic of Korea

References

[1] A. Elgawadi, J. Krasinski, G. Gainer et al., "Modification of the anomalous optical transitions in multilayer AlGaN-based nanoheterostructure using a nonbonding laser lift-off technique," J Appl Phys 103 (12), 123512 (2008).

[2] Y. G. Tian and Y. C. Shin, "Laser-assisted machining of damage-free silicon nitride parts with complex geometric features via in-process control of laser power," J Am Ceram Soc 89 (11), 3397-3405 (2006).

[3] N. Muhammad, D. Whitehead, A. Boor et al., "Picosecond laser micromachining of nitinol and platinum-iridium alloy for coronary stent applications," Appl Phys a-Mater 106 (3), 607-617 (2012)

[4] E. Gu, C. W. Jeon, H. W. Choi et al., "Micromachining and dicing of sapphire, gallium nitride and micro LED devices with UV copper vapour laser," Thin Solid Films 453, 462-466 (2004).

[5] P. Molian, B. Pecholt, and S. Gupta, "Picosecond pulsed laser ablation and micromachining of 4H-SiC wafers," Appl Surf Sci 255 (8), 4515-4520 (2009).

[6] G. Y. Mak, E. Y. Lam, and H. W. Choi, "Interconnected alternating-current light-emitting diode arrays isolated by laser micromachining," J Vac Sci Technol B 29 (1) (2011)

[7] K. N. Hui, X. H. Wang, Z. L. Li et al., "Design of vertically-stacked polychromatic light-emitting diodes," Opt Express 17 (12), 9873-9878 (2009).

[8] W. Y. Fu, K. N. Hui, X. H. Wang et al., "Geometrical Shaping of InGaN Light-Emitting Diodes by Laser Micromachining," IEEE Photonics Technol Lett 21 (15), 1078-1080 (2009).

[9] K. N. Hui, K. S. Hui, H. Lee et al., "Enhanced light output of angled sidewall light-emitting diodes with reflective silver films," Thin Solid Films 519 (8), 2504-2507 (2011).

[10] K. N. Hui and K. S. Hui, "Vertically-stacked LEDs with invariance of color Chromaticity," Curr Appl Phys 11 (3), 662-666 (2011).

[11] X. H. Wang, P. T. Lai, and H. W. Choi, "Laser micromachining of optical microstructures with inclined sidewall profile," J Vac Sci Technol B 27 (3), 1048-1052 (2009).

[12] G. Y. Mak, E. Y. Lam, and H. W. Choi, "Precision laser micromachining of trenches in GaN on sapphire," J Vac Sci Technol B 28 (2), 380-385 (2010).

[13] K. J. Vampola, M. Iza, S. Keller et al., "Measurement of electron overflow in 450 nm InGaN light-emitting diode structures," Appl Phys Lett 94, 061116 (2009).

[14] J. J. Wierer, D. A. Steigerwald, M. R. Krames et al., "High-power AlGaInN flip-chip light-emitting diodes," Appl Phys Lett 78, 3379-3381 (2001).

[15] S. J. Park, M. K. Kwon, J. Y. Kim et al., "Enhanced emission efficiency of GaN/InGaN multiple quantum well light-emitting diode with an embedded photonic crystal," Appl Phys Lett 92, 251110 (2008).

[16] C. H. Kuo, C. M. Chen, C. W. Kuo et al., "Improvement of near-ultraviolet nitride-based light emitting diodes with mesh indium tin oxide contact layers," Appl Phys Lett 89, 201104 (2006).

[17] C. C. Kao, H. C. Kuo, H. W. Huang et al., "Light-output enhancement in a nitride-based light-emitting diode with 22 degrees undercut sidewalls," IEEE Photonics Technol Lett 17 (1), 19-21 (2005).

[18] F. K. Yam and Z. Hassan, "Innovative advances in LED technology," Microelectron J 36 (2), 129-137 (2005).

[19] L. Zhu, X. H. Wang, P. T. Lai et al., "Angularly Uniform White Light-Emitting Diodes Using an Integrated Reflector Cup," I IEEE Photonics Technol Lett 22 (7), 513-515 (2010).

[20] C. Hoelen, J. Ansems, P. Deurenberg et al., "Color tunable LED spot lighting, " SPIE 6337, 63370 (2006).

[21] J. K. Sheu, S. J. Chang, C. H. Kuo et al., "White-light emission from near UV InGaN-GaN LED chip precoated with blue/green/red phosphors," IEEE Photonics Technol. Lett. 15 (1), 18-20 (2003).

[22] G. Heliotis, P. N. Stavrinou, D. D. C. Bradley et al., "Spectral conversion of InGaN ultraviolet microarray light-emitting diodes using fluorene-based red-, green-, blue-, and white-light-emitting polymer overlayer films," Appl Phys Lett 87, 103505 (2005).

[23] Y. Xuan, D. C. Pan, N. Zhao et al., "White electroluminescence from a poly(N-vinylcarbazole) layer doped with CdSe/CdS core-shell quantum dots," Nanotechnology 17, 4966-4969 (2006).

[24] Narendran, N, Maliyagoda, N, & Deng, L. et al., "Characterizing LEDs for general illumination applications: Mixed-color and phosphor-based white sources," SPIE 4445, 137-147 (2001).